Linköping Studies in Science and Technology
Licentiate Thesis No. 2017

Thermoelectric properties of CrN alloy thin films

Victor Hjort

LINKÖPING UNIVERSITY

Linköping Studies in Science and Technology
Licentiate Thesis No. 2017

Thermoelectric properties of CrN alloy thin films

Victor Hjort

Thin Film Physics Division
Department of Physics, Chemistry, and Biology (IFM)
Linköpings universitet, SE-581 83 Linköping, Sweden
Linköping 2025

Supervisor:
Per Eklund
Professor
Department of Chemistry – Ångström Laboratory, Uppsala University
Department of Physics, Chemistry and Biology, Linköping University

Co-supervisors:
Arnaud le Febvrier
Researcher, Docent
Department of Chemistry – Ångström Laboratory, Uppsala University
Department of Physics, Chemistry and Biology, Linköping University

Fredrik Eriksson
Associate Professor, Docent
Department of Physics, Chemistry and Biology, Linköping University

Faculty opponent:
Tomas Nyberg
Associate Professor, Docent
Department of Electrical Engineering, Uppsala University

Printed in Sweden by LiU-tryck, 2025

ISBN 978-91-8118-075-6 (Tryckt)
ISBN 978-91-8118-076-3 (PDF)
https://doi.org/10.3384/9789181180763
ISSN 0280-7971

Abstract

A thermoelectric material can be used to convert heat to electricity, and vice versa, all without moving parts. Thermoelectric devices can be used for a multitude of applications, such as thermoelectric generators (TEGs) and Peltier heaters/coolers. TEGs can be used to generate electricity from e.g. waste heat, and small and efficient Peltier coolers could have a use in microelectronics. The lack of moving parts means that thermoelectric devices generally are robust.

Transition metal nitrides are versatile, durable, and have found use in many different applications. CrN, for instance, is known for its hardness, corrosion resistance, near room-temperature magnetic phase transition as well as its thermoelectric properties. Especially crystalline CrN has interesting thermoelectric properties, including a high power-factor and low thermal conductivity. These properties are essential for the constituent materials of thermoelectric devices. For durability, the stability and mechanical properties of CrN would be a bonus. The thermoelectric properties of CrN have a strong correlation to the stoichiometry, which then becomes crucial to control.

The focus of this thesis is on the thermoelectric properties of CrN, with and without alloying transition metals V and Mo. Doping and alloying can help change properties, both electrical and thermal. I have grown thin films of CrN with and without alloying elements, using reactive magnetron sputtering. Film growth using this technique happens far from thermodynamic equilibrium and thus, not all aspects are easy to control, stoichiometry being one. The films were grown on c-plane sapphire (Al_2O_3 (0001)) substrates.

I investigated thin, epitaxial films of CrMoVN, i.e. CrN thin films co-doped with Mo and V. They were grown on c-plane sapphire substrates, which allows the rock-salt cubic structured CrN to be grown epitaxially, albeit with a non-negligible strain. I investigated the effect of co-doping on phase composition and thermoelectric properties. While the effects of singly doped films (CrVN and CrMoN) were similar to other reports, co-

doping with V and Mo resulted in the retention of the rock-salt cubic phase at much higher Mo-content than what has previously been reported. Furthermore, I tackled the issue with stoichiometry, motivated by discrepancies in literature correlating thermoelectric properties and stoichiometry of CrN. After growing sets of thin films of CrN, some epitaxial and some mix-phased, the samples were annealed in ammonia environment to approach the thermodynamic equilibrium of Cr:N = 1:1. The films that were closest to stoichiometry before annealing turned insulator – in line with theory and some articles. The films with larger under-stoichiometry got significantly improved thermoelectric properties, one by as much as 900%.

Keywords: Thermoelectrics, CrN, Magnetron sputtering, Thin films, Epitaxy

Populärvetenskaplig sammanfattning

Ett termoelektriskt material kan användas för att omvandla värme till elektricitet, och vice versa, helt utan rörliga delar. Termoelektriska enheter kan användas för en rad olika tillämpningar, såsom termoelektriska generatorer för att generera elektricitet från exempelvis spillvärme, och Peltier-element för uppvärmning eller kylning för t.ex. mikroelektronik eller bilsäten. Avsaknaden av rörliga delar gör att termoelektriska enheter i allmänhet är robusta.

Övergångsmetallnitrider är mångsidiga, ofta hållbara, och har flera olika användningsområden. CrN (kromnitrid), till exempel, är känt för sin hårdhet, korrosionsbeständighet, en magnetisk fasövergång nära rumstemperatur och sina termoelektriska egenskaper. Särskilt kristallint CrN har intressanta termoelektriska egenskaper, inklusive en hög effektfaktor och låg värmeledningsförmåga - egenskaper som är avgörande för termoelektriska material. Stabiliteten och de mekaniska egenskaperna hos CrN ger en extra fördel om termoelektriska enheter baseras på CrN. Det finns en stark korrelation mellan CrNs termoelektriska egenskaper och dess stökiometri, vilket gör det avgörande att kunna kontrollera sammansättningen.

Denna avhandling fokuserar på de termoelektriska egenskaperna av tunna filmer av CrN, med och utan legering. Dessa filmer har skapats genom reaktiv magnetronsputtring - en teknik som sker långt från termodynamisk jämvikt, vilket innebär att vissa aspekter, som stökiometri, är svåra att kontrollera.

Jag har undersökt tunna filmer av CrMoVN, det vill säga CrN-filmer som var dopade med både Mo (molybden) och V (vanadin), och har undersökt effekter av stökiometri genom att skicka tunna filmer av CrN, vissa epitaxiella och vissa med blandade faser, för värmebehandling i ammoniakmiljö för att komma närmare den termodynamiska jämvikten Cr:N = 1:1. De filmer som var närmast stökiometriska innan värmebehandlingen blev isolatorer medan filmerna med lägre kvävehalt fick signifikant förbättrade termoelektriska egenskaper.

Preface

This licentiate thesis is a part of my Ph.D. studies in the Energy Materials unit in the Thin Film Physics Division at the Department of Physics, Chemistry, and Biology (IFM), at Linköping University.

This work has been supported by the Swedish Government Strategic Research Area in Materials Science on Functional Materials at Linköping University (Faculty Grant SFO-Mat-LiU No. 2009 00971), the Knut and Alice Wallenberg foundation through the Wallenberg Academy Fellows program (grant no. KAW-2020.0196), the Swedish Research Council (VR) under project no. 2021-03826, and the Swedish Energy Agency under project number 52740-1. I have been enrolled in the graduate school Agora Materiae.

Linköping, 2025
Victor Hjort

Acknowledgements

I wish to extend my gratitude to everyone who have supported and helped me towards my licentiate at Linköping University. To name a few:

A big thank you to my main supervisor **Per Eklund**, for support and understanding, the always swift and thorough feedback, and for showing me the true meaning of *efficiency*.

A big thank you to my co-supervisor **Arnaud le Febvrier** for great support and trust regarding everything from vacuum systems to diffractometers. Also, for all early input on manuscript and explaining how to express one's research, in writing and in figures. Thank you to my second co-supervisor **Fredrik Eriksson** for without hesitation agreeing to being my in-house support.

Thank you everyone around IFM whom I have shared interesting conversations with, scientific or other. Especially big thank you; **Johan Nyman**, for welcoming every newcomer, and for helpful discussions in the lab and during ion-beam analysis; **Justinas Palisaitis** for great help in anything regarding TEM; **Thomas Lingefelt** for quick support for anything lab-related; **Per Sandström** for help in the lab.

Thank you, **Rui Shu** and **Smita Rao,** for the great support of a new, slightly confused researcher. And, to the rest of the members of my previous unit, Energy materials unit, **Faezeh**, **Niraj**, **Susmita**, **Sanath** and **Sagar** for interesting discussions. Thanks to all **Agora Materiae members**, and **Caroline Brommeson** for the great organization of the Agora activities. Thank you **Kenneth Järrendahl** for letting me join the Materials optics unit when my previous unit got disbanded.

Stort tack till mina kontorsgrannar, **Marcus Lorentzon** och **Anton Zubayer**, för trevliga diskussioner och gott sällskap, trots våra olika tidszoner.

Och så ett särskilt stort tack till min kära fru för ditt konstanta stöd.

Details of included papers

Paper I

Phase Composition and Thermoelectric Properties of Epitaxial CrMoVN Thin Films

Authors: Victor Hjort, Niraj Kumar Singh, Susmita Chowdhury, Rui Shu, Arnaud le Febvrier, Per Eklund

Adv. Energy Sustain. Res., vol. 4, no. 12, p. 2300119, 2023

Author's contribution: I was responsible for planning and conceptualization, from choosing materials to performing the depositions. I did most of the analysis and characterization and I wrote the manuscript.

Paper II

Influence of Ammonia Annealing on Cr–N Thin Films and Their Thermoelectric Properties

Authors: Victor Hjort, Franck Tessier, Fabien Giovannelli, Arnaud le Febvrier, Per Eklund

ACS Appl. Energy Mater., vol. 7, no. 15, pp. 6785–6792, 2024

Author's contribution: I was responsible for planning and conceptualization. I did the depositions, most of the analysis, and I wrote the manuscript.

Papers not included in the thesis

Thermoelectric properties and electronic structure of Cr(Mo,V)N_x thin films studied by synchrotron and lab-based x-ray spectroscopy

Authors: Susmita Chowdhury, Victor Hjort, Rui Shu, Grzegorz Greczynski, Arnaud le Febvrier, Per Eklund, Martin Magnusson

Phys. Rev. B, vol. 108, no. 20, p. 205134, 2023

Effects of W alloying on the electronic structure, phase stability, and thermoelectric power factor in epitaxial CrN thin films

Authors: Niraj Kumar Singh, Victor Hjort, Sanath Kumar Honnali, Davide Gambino, Arnaud le Febvrier, Ganpati Ramanath, Björn Alling, Per Eklund

J. Appl. Phys., vol. 136, no. 15, p. 155301, 2024

Enhanced upper critical fields for superconductivity in strain-engineered molybdenum nitride thin films

Authors: Aditya Singh, Divya Rawat, Victor Hjort, Subhankar Bedanta, Arnaud le Febvrier, Per Eklund, Ajay Soni

In manuscript

Table of Contents

Chapter 1

1 Introduction

Energy. A word and concept everyone has a daily connection with. Whether one thinks of one's need for coffee, the accompanying energy-packed *fika*, the thick black liquid pumped up from seabeds, or the constant political debate regarding wind or nuclear power plants, energy is all around us, and our needs of it seem to be ever-increasing. Consequently, we continue burning fossil fuels even though it is a major cause of global warming and its rapidly increasing effects. To reevaluate our needs for energy, on a grand scale and in the modern world, is difficult, if not impossible. Accepting the increasing energy demand, one focus for fulfilling the Paris agreement[1] should be on renewable energy sources. But, in 2016 it was estimated that 70% of the world's energy consumption is lost as waste heat.[2] Another focus must thus be on improving the efficiency of already existing products. Thermoelectricity is the conversion of energy from heat to electricity, and vice versa. This renders harvesting of waste heat, and thus increasing the efficiency of existing systems, a possible application for thermoelectric devices.

The basic principle of thermoelectric materials is that when a conducting material is subjected to a temperature gradient, its charge carrier will start diffusing from the warm to the cold side. As the charge carriers accumulate on the cold side, there will be a potential difference over the two ends. Reversing the process by applying a voltage will instead cause a temperature difference, known as the Peltier effect. Regardless, the material needs to have a low thermal conductance to maintain the temperature gradient.[3] For semiconductors, charge carriers can be either electrons (n-type) or holes (p-type).[4] By connecting several p- and n-type thermoelectric legs in series, such as in Figure 1, either a current can be drawn (energy harvesting) or a temperature difference can be created (Peltier heating/cooling). Thermoelectric devices can be made small and have no moving parts. The latter is a major bonus for making robust devices.

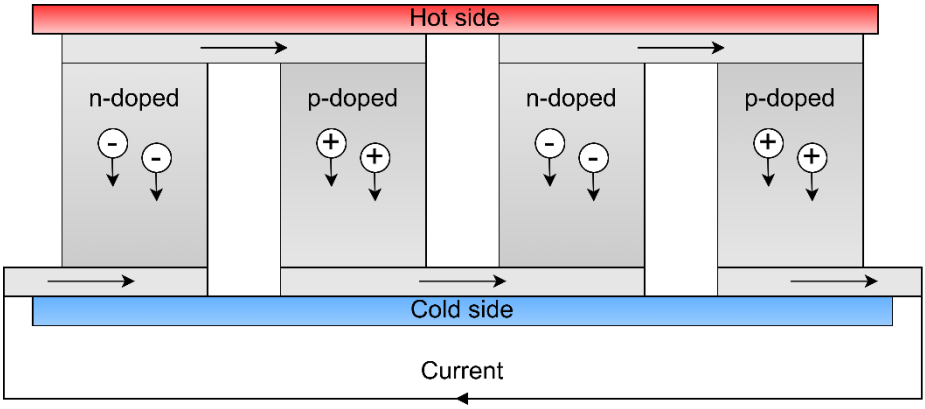

Figure 1. Schematic of a simple thermoelectric device. Image from Rutberg.[5]

Commercialized thermoelectric devices are often telluride-based. Tellurium is very scarce, making this choice expensive and not suitable for large-scale manufacturing. One of the promising materials to replace tellurides in thermoelectric devices is chromium nitride (CrN). Chromium is abundant in the earth's crust, and nitrogen comprises most of the air in the atmosphere. CrN is a semiconductor with a power factor on par with that of tellurides (1-10 $mWm^{-1}K^{-2}$)[6–9], a low thermal conductivity (2-4 $Wm^{-1}K^{-1}$), compared to similar material.[9–13] Furthermore, CrN can be made n- or p-type, depending on stoichiometry and alloying elements.[14,15] These factors makes CrN an promising choice for future thermoelectric devices.

The aim of this thesis is to investigate means of altering the Cr-N materials system to improve its thermoelectric properties and bringing this environmentally friendly materials system a few steps towards practical thermoelectric devices.

2 Thin film deposition and growth

The word “thin” in thin films usually means films with thickness ranging from some nanometers to a few micrometers. Depending on the film’s thickness, composition, microstructure, impurities, and more, a multitude of different properties can be achieved. The films can be insulating, conducting, or semiconducting, be soft or flexible, or have interesting optical properties.[16] Thin films are commonly used as coatings for applications such as hard coatings for cutting tools, and as corrosion resistance for materials placed in harsh environments.[17–21] For hard coatings, thin films are often (x-ray) amorphous or polycrystalline, while thin films used as semiconductors have a high crystal quality, often single-crystal with few defects.[4]

Deposition refers to the change of state of matter directly from gas to solid state, instead of condensation (gas to liquid) followed by freezing (liquid to solid). Where the films are being deposited is often simply referred to as the substrate. Two common categories of techniques for thin film deposition are Physical Vapor Deposition (PVD) and Chemical Vapor Deposition (CVD). In CVD, precursor gases are introduced into a reaction chamber. There they react with the heated substrate, depositing a solid material. What is left are various gases (by-products) which are vented from the chamber. An example is the use of silane gas (SiH_4) or trichlorosilane ($SiHCl_3$) to deposit Si.[4] PVD techniques, in one way or the other, vaporize the (solid or sometimes liquid) source material, which is then transferred to the substrate where it is deposited. Regardless of the techniques, a strict control of the environment is necessary. For one thing, controlling the properties of the grown film. For certain materials, presence of impurities can cause the synthesized material to have completely different properties.[4] But also because most techniques would not work otherwise. Environmental control is achieved by vacuum chambers.

2.1 Vacuum and materials science

The areas of vacuum and materials science are forever intertwined. It was not until Guericke did his famous experiment with the Magdeburg hemispheres (which two teams of eight horses just barely pulled apart)[22] that people were getting convinced of the existence of vacuum. Since vacuum was discovered, scientists have continuously been trying to improve vacuum technology. In the beginning it was mainly a question of engineering, such as inventing and developing pumps. Soon, the materials themselves would show limits on how good vacuum one can get, and further analysis of the materials used was needed. In turn, vacuum and vacuum chambers have been an essential part of materials science during the last century.

When high control of the environment is needed, such as growing thin films with low number of impurities, one needs to be in the ultra-high vacuum (UHV) regime. UHV means a pressure in the range of 10^{-5}-10^{-9} Pa, or around 10^{-7}-10^{-11} Torr. The latter is a unit named after Evangelista Torricelli, who is one of two people (the other is Gasparo Berti) who independently demonstrated that a glass tube full of mercury, turned upside down in a mercury reservoir, drops down 76 cm.[22] Hence the unit 1 atm (atmosphere) = 760 mmHg = 760 Torr. To reach UVH pressures, the vacuum system needs to have no leaks, the walls must have low permeability and have a high degassing rate from the surface. To achieve no leaks, every connection, feedthrough and surface needs to be properly sealed and prepared. One can use bellows, magnets, and various fluids to ensure no leaks while allowing translational and rotational motion inside the chamber.[23] Flanges are often ConFlat® knife edges which compress a soft metal (often copper) to seal the connection. The chamber walls are made of either low carbon-stainless steel or aluminum. Several pumps are needed to reach UHV because common pumps such as the turbomolecular pump (or just turbopump or turbo) only works under 1 Pa ($<10^{-2}$ Torr). Thus, a turbo requires a backing pump to help pump down from atmospheric pressure. Similarly, several gauges are needed to evaluate the chamber vacuum level, as different gauges have different working range.[23]

Lower pressure means fewer residuals/contaminants, and a higher mean-free path of any molecule. For anything involving, e.g., electron beams (such as electron microscopes), a large mean-free path is crucial. Vacuum, or at the very least control of the environment, is also needed for other characterization techniques, such as X-ray Photoelectron Spectroscopy (XPS)[24] and various high-temperature measurements.

2.2 Sputtering

The simplest form of sputtering, *diode sputtering*, has three components: a sputtering gas (commonly argon), a cathode (where the target material, to be sputtered, is placed), and an anode. Of course, a power supply to create a potential at the cathode is also needed. The cathode and sputtering gas are put inside a vacuum chamber while the vacuum chamber itself acts as the anode in the sputtering process.

Sputtering works 1. By employing a large negative voltage over the cathode, the sputtering gas is ignited to create a plasma. This means that the atoms in the sputtering gas are excited to the point that their outermost electrons leave their electron shells, leaving positive ions and negative electrons floating around in an energetic sea of charges. In sputtering processes, only a small fraction (a few percent) of the sputtering gas is ionized. 2. The positive ions are attracted to the target by the large negative potential of the cathode. 3. Some of the impinging ions will be lodged inside the target and some will be scattered away, but by a game of atomic billiards, most will cause a chain reaction in the target which in one way or other causes atoms from the target to be ejected in a ballistic fashion. 4. Atoms and electrons leave the target. While some (atoms) pass through the plasma, some of the ejected particles will cause further ionization of the sputtering gas, keeping the plasma ignited. 5. The atoms that make their way through the sputtering gas and reach the substrate, or any solid in the chamber. The atoms are adsorbed on the surface and will move around until they find a metastable position or until they are desorbed again. The highest flux of ejected atoms is normal to the target, which is why the substrate is placed normal to the target. An addition to the current section is that without

any ionized atoms, a high voltage of a few 100 V would not be able to ignite a plasma. It needs a starting point. Thanks to the background radiation, there will always be a few ionized atoms in the chamber, which upon applying a voltage causes a chain reaction: the plasma is running!

2.2.1 Magnetron Sputtering

Like diode sputtering, magnetron sputtering utilizes a sputtering gas, a cathode, and an anode. The addition of a magnetron greatly improves the process. By placing a magnetron behind the target (see Figure 2), the magnetic field from the magnetron forces the ejected electrons to be trapped near the target, causing them to hit and ionize more atoms, a reaction described in eq. (1). This entrapment in turn causes the plasma to be confined closely above the target, which greatly increases the sputtering rate, compared to diode sputtering. The force acting upon the moving electrons is called the Lorentz force, described in eq. (2)

$$e^- + Ar = 2e^- + Ar^+ \tag{1}$$

$$\bar{F} = q(\bar{E} + \bar{v} \times \bar{B}) \tag{2}$$

Many lab-scale magnetrons are circular, comprising of one center magnet and a ring of outer magnets, with the center magnet being reversed polarity of that of the outer ring. The highest concentration of electrons, and positive ions, will be where the magnetic field lines are perpendicular to the cathode. Because of this, a characteristic racetrack will be seen on a target used for magnetron sputtering. This is because the target will be sputtered away faster right under where the plasma is most dense.[25]

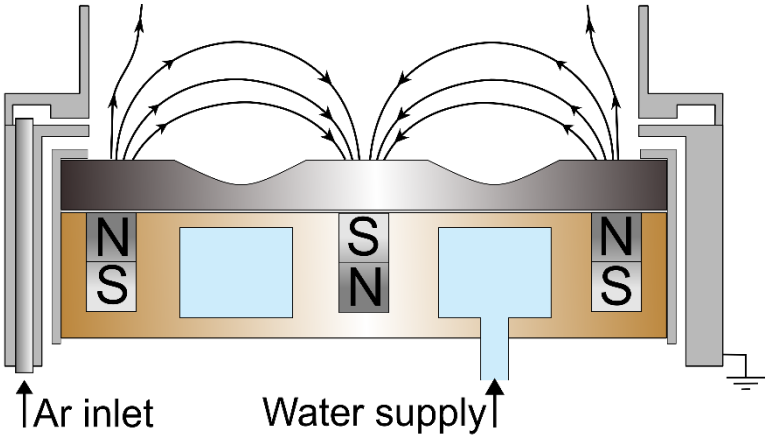

Figure 2. Schematic of a magnetron for magnetron sputtering. Seen are magnetic field lines, magnets, target and water-cooled Cu-backing plate behind it.

2.2.2 Reactive Sputtering

In reactive magnetron sputtering, one adds a *reactive* gas to the chamber, in addition to the sputtering gas. This is a common way to make oxides (add O_2) and nitrides (add N_2). Upon addition of e.g. N_2, nitrides will be formed on *every surface* inside the vacuum chamber, which includes the substrate as well as the target. As more of the surface forms compounds with the reactive gas, the electrical properties of the target will change. For metallic targets, the electrical conductivity will *likely* decrease, and if so, increase the potential at the target. This reduces the attraction of the sputtering gas which in turn lowers the deposition rate. For some materials and reactive gas flow, inserting a reactive gas could lead to an insulating surface layer which can stop the sputtering process. The relationship between reactive gas flow and sputter rate, as well as to reactive gas pressure, is non-linear and hysteresis is commonly observed.[26] Comparing with Figure 3, one has reached poisoning mode after the sudden increase in pressure (and drop in sputtering rate), and it is desired to stop increasing the gas flow before poisoning happens. Ideally, one wants to maintain a high sputter rate and as high reactive gas flow as possible, since a higher reactive gas flow means that the grown film will have a higher content of the reactive gas.

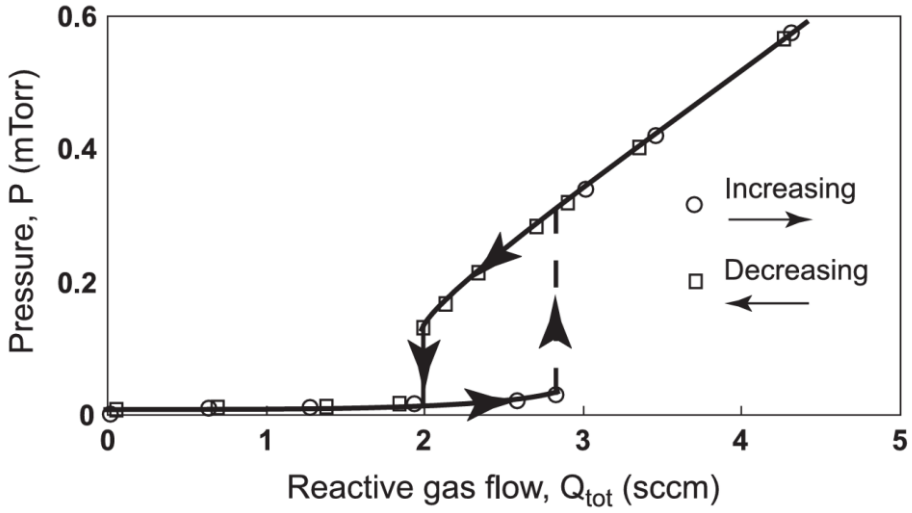

Figure 3. Hysteresis of reactive gas flow vs. partial pressure. Image from Berg and Nyberg.[26] © Elsevier, reproduced with permission.

2.3 Thin Film Growth

Thin film growth by PVD techniques means deposition of particles in vapor phase onto a substrate. The two most important factors, besides what material and substrate one uses, are substrate temperature and energy of the impinging particles. Regardless of the temperature at the substrate, the vapor phase will have a much higher temperature. This means rapid quenching, and deposition, onto the substrate. In turn, this means that the deposition process occurs far from thermodynamic equilibrium, allowing metastable phases to be grown. With increasing substrate temperature, an increased adatom mobility follows, i.e. the atoms move around on the surface for a longer time, allowing them to find more energetically favorable positions before they finally stick. Thus, larger crystallites often follow with increasing substrate temperature. The downside of increasing the substrate temperature (besides energy consumption) is that it can be a large source of strain in the film, because of the often-different thermal expansion coefficients of the substrate and the film. Forcing the film and substrate to match at several hundred degrees above room temperature will likely cause the much thinner film to be strained at room temperature.

The three basic growth modes for films on substrates are Volmer-Weber (island growth), Frank-van der Merwe (layer-by-layer growth) and Stranski-Krastanov. The latter describes an initial layer-by-layer growth followed by island growth after a critical thickness. These three growth modes are illustrated in Figure 4. Which growth mode occurs is explained by strain from the three interfaces: substrate-vapor, substrate-film, and film-vapor.[27]

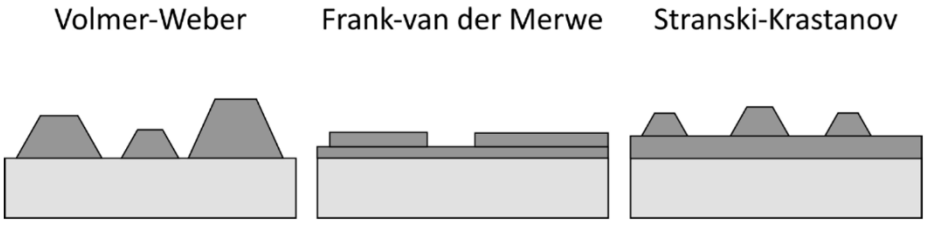

Figure 4. An illustration of the three growth modes. Image from Lorentzon.[28]

2.3.1 Crystals and ordering

The crystallites in the grown film can be randomly oriented, uniaxially textured, or biaxially textured. Randomly oriented films have no in- or out-of-plane ordering of the crystallites. In uniaxially textured (fiber-textured) films the crystallites are ordered along one direction but not the other. For thin films this usually means that the out-of-plane orientation is the same for all crystallites, while the in-plane orientation is randomly distributed. If the in-plane directions of the crystallites are also ordered, one talks of biaxially textured films. For thin films this usually means epitaxial growth. For many fields within materials science, epitaxial growth means at the very least that the individual crystallites are epitaxially related to the substrate, and not necessarily single-crystal epitaxial growth. For visualization of these three orientations, see Figure 5. Choosing material system with matching high-quality substrate, the film grows epitaxially with the substrate crystal as a model.[4]

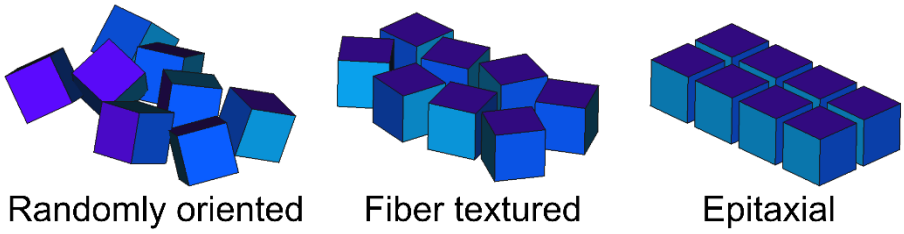

Figure 5. Illustration of randomly oriented, fiber textured, and epitaxial ordering of crystallites.

To describe a crystal, one needs both a lattice and a basis. A lattice is an infinitely repeating pattern, and a base can be one or several atoms. Crystals are thus solid materials with long-range order. The simplest lattice is the cubic, with right angles and equally long principal axes. The three cubic systems are simple cubic (sc), face-centered cubic (fcc), and body-centered cubic (bcc).[29] These three are illustrated in Figure 6.

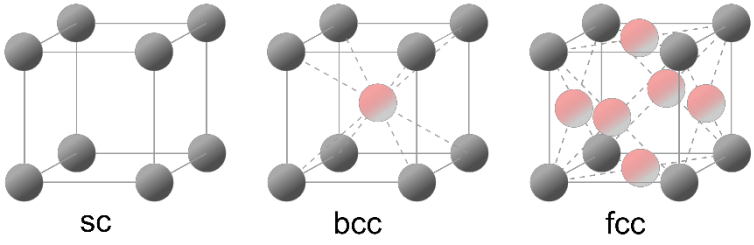

Figure 6. Illustration of the three cubic systems, simple cubic (sc), face-centered cubic (fcc), and body-centered cubic (bcc).

We use Miller indices, *hkl*, to label planes and directions in crystals. For hexagonal structures (and hexagonal-like structures, such as Al_2O_3), one likes to use four indices, *hkil*. This is called the Bravais-Miller system. The extra index is redundant, since $h + k + i = 0$, but helps in visualization.

The ideal substrate is the material itself, e.g. growing Si film on Si-substrate, which is referred to as homoepitaxy. In most cases, the desired thin film material is not available as substrate, and homoepitaxy is not feasible. One way to grow epitaxial films is choosing a substrate with the

same crystal structure and similar cell parameters, such as growing CrN on MgO substrate.[14] Another is finding a suitable substrate by matching a specific plane of a crystal with the desired material system. One match for rock-salt cubic structures such as CrN is c-plane sapphire (Al_2O_3 (0001)), which promote growth of CrN (111).[30] The grown film will have more defects if the lattice mismatch between film and substrate is large.

3 Thermoelectrics

Thomas Johann Seebeck discovered the Seebeck effect in 1821.[3] Although, others, such as Andrea Volta, also contributed to this field before Seebeck.[31] Seebeck found that if one places two dissimilar metal wires into contact, and heat this junction, one can measure a voltage over the loose ends. Jean Peltier discovered the reverse effect: if one in the same setup gives a potential difference over the two ends, the temperature at the junction will change. William Thomson (later Lord Kelvin) realized that these two effects are connected and showed it through thermodynamic relations. He also found that if there is both an electric and a thermal current, the material will either heat up or cool down depending on the currents relative flow directions, known as the Thomson effect.[3] Together, these three factors comprise the thermoelectric effect. From Thomson's work, the two branches of physics, thermodynamics (Fourier's law) and electrodynamics (Ohm's law), were merged. If a material is subjected to a temperature difference, Fourier's law tells that with a temperature difference follows a heat flux from hot to cold. In solids, there are two main aspects of heat transfer: through the lattice (which in crystals are mediated by phonons) and through charge carriers.[29]

The most basic thermoelectric device is a thermocouple, which consists of one n-type and one p-type wire fused together at one end. Such a pair of n- and p-type thermoelectric material is referred to as a pair of legs. A single pair of legs will not render a high voltage or power and for energy harvesting, or for Peltier modules, several legs are connected in series to amplify its effect. The holes and electrons from the p- and n-type legs, respectively, recombine at the cold side and a current can continuously be drawn. An illustration of such a thermoelectric device is seen in Figure 1.

There are three main aspects of a good thermoelectric material: high electrical conductivity (σ), low thermal conductivity (κ), and a high Seebeck coefficient (S), which together form two important factors. One is the *dimensionless figure of merit* (zT, eq. (3)), which is a measure of efficiency. The other important factor is referred to as the power factor (P_F, eq. (4)). P_F is the numerator in zT and is a measure of power output. T stands for temperature. A thermoelectric device is, in essence, a heat engine. Thus, one must consider the fundamental thermodynamic limitation of the Carnot cycle when talking of efficiencies. Without the two irreversible effects of Fourier diffusion (heat diffuses from hot to cold) and Joule heating (a current that passes through a conductor produces heat), the efficiency would be at the Carnot limit value (eq. (5)). Instead, the total efficiency boils down to eq. (6). Here, ZT_M is the *thermocouple* dimensionless figure of merit at the average temperature, T_M.[3] I.e. the efficiency for a pair of thermoelectric legs. It can be shown that the transport properties of the n- and p-type legs should match for optimal ZT. Consequently, matching two materials with the highest zT doesn't necessarily give the best *device* performance.[3] Parasitic electrical losses from contacts, thermal losses, different thermal expansion coefficients, diffusion barriers (the elements of the thermoelectric material, and nothing else, should stay in the legs), mechanical properties (high hardness for handling mechanical stress, or maybe flexibility?), number of legs (higher voltage vs. higher internal resistance), size (length and area) of each leg, and arrangement of the individual legs (series, or perhaps in cascade?), among others, are design factors that determines the device performance.[3,32–35]

$$zT = \frac{\sigma S^2}{\kappa} T \tag{3}$$

$$P_F = \sigma S^2 \tag{4}$$

$$\eta_c = \frac{\Delta T}{T_H} \tag{5}$$

$$\eta^* = \eta_c \frac{\sqrt{1+ZT_M}-1}{\sqrt{1+ZT_M}+\frac{T_C}{T_H}} \quad (6)$$

S (unit VK^{-1}), σ (Sm^{-1}), and κ ($Wm^{-1}K^{-1}$) can be described as stated below, in eq. (7)-(9), and T stands for temperature (K). Electrical resistivity, ρ (Ωm), is related to electrical conductivity by $\sigma = \rho^{-1}$. With the Seebeck coefficient being squared in both zT and P_F, small differences in S can make a large difference for both efficiency and power output. The Seebeck coefficient of metals and degenerate semiconductors can also be expressed in fundamental material parameters, as seen in eq. (10).[36]

$$S = \frac{\Delta V}{\Delta T} = \frac{V_C - V_H}{T_H - T_C} \quad (7)$$

$$\sigma = en\mu \quad (8)$$

$$\kappa = \kappa_e + \kappa_p = L\sigma T + \kappa_p \quad (9)$$

$$S = \frac{8\pi^2 k_B^2}{3eh^2} m^* T \left(\frac{\pi}{3n}\right)^{\frac{2}{3}} \quad (10)$$

Here, V is voltage (at cold or hot side), e is elementary charge, h is Planck's constant, n is the charge carrier concentration, μ is the mobility of these charge carriers, κ_e and κ_p are the electrical and lattice contribution to the thermal conductivity, respectively, L is the Lorenz number, k_B is Boltzmann's constant, m^* is effective mass. The three parameters S, σ, and κ are interdependent, which is clear from equations (7)-(10) above. Managing to alter one of them often means that the other two are affected as well. For instance, S, σ, and κ all depend on charge carrier concentration, and as seen in Figure 7, this dependency renders a maximum for zT.[36] A deeper insight into how the various parameters affecting zT are related is given in Figure 8.[37]

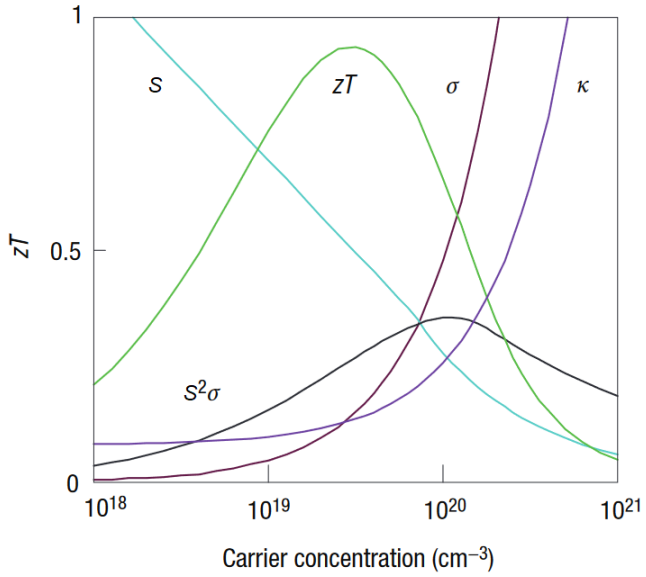

Figure 7. How zT, S, σ, and κ are related to charge carrier concentration. Image adapted from Snyder and Toberer.[36] © Springer Nature, reproduced with permission.

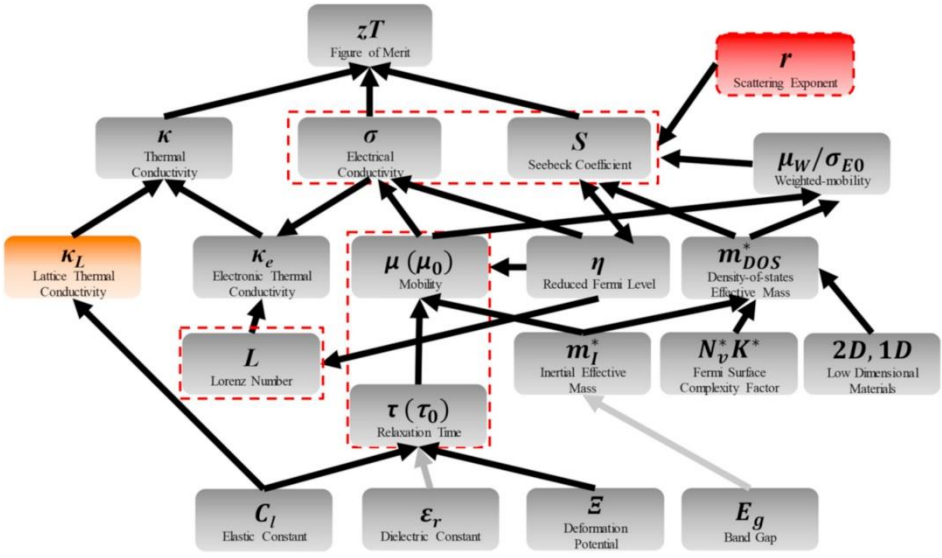

Figure 8. Some interdependencies of the thermoelectric properties. Image from Jia et al. [37] © Elsevier, reproduced with permission.

Application areas for thermoelectrics are heat-to-energy-conversion (thermopile or thermoelectric generator, TEG), and for creating a

temperature difference (Peltier heating/cooling). TEGs have found use in areas from heat-distributing fans on top of soapstone ovens to space missions.[38] Future applications could be wherever there is waste heat. Peltier heaters/cooling can be used for controlling the temperature. While the efficiency is too low for large scale heating/cooling[39], it can be found in e.g. picnic coolers or for local temperature control, in places such as lab equipment or microelectronics.

Typical materials used today are tellurides of bismuth, antimony, and lead, among others.[6,7,35,36,40–42] These elements are expensive, scarce, and mostly toxic, which is one reason for searching for other thermoelectric materials. The most simple and common thermoelectric device, the thermocouple, often consists of the two alloys chromel and alumel (known as a K-type thermocouple). These alloys consist of relatively cheap and abundant materials (mainly nickel, chrome, and aluminium) but have too low zT to be of much use outside of temperature measurements. When determining the Seebeck coefficient of materials, platinum is often used as a reference. All metals (above superconducting temperatures) have thermoelectric properties. For example, platinum has a Seebeck coefficient of around -5 μV/K at room temperature.[43]

3.1 Improving thermoelectric properties

For decades, several strategies have been employed to improve the thermoelectric properties of existing materials. They sum up to means of altering transport properties of charge carriers or phonons (for crystals). This can be done by e.g. altering charge carrier density or mobility[44], or by focusing on phonon properties.[36,45] Doping or alloying will affect the charge carrier density and increasing the disorder will increase the phonon scattering, which means a reduction of thermal conductivity. Disorder in the crystal structure can also be incorporated by e.g. nanostructuring[46–48], inclusions of secondary phases[49], or by voids caused by ion implantation[50]. While disorders in the crystal hinders phonon propagation, such disorders will in most cases also affect the transport properties of charge carriers. Interfaces such as grain boundaries are a large source for charge carrier scattering and a

reduction of electrical conductivity thus follows with increasing number of grain boundaries. The ideal case would be a so-called phonon-glass/electron-crystal, a thermally insulating and electrically conducting material.[48,51,52] While novel thermoelectric materials can comprise of completely new elements, more often the novelty comes from clever variations and nanostructures or simply going from bulk materials to lower dimensions.[53] For low dimension materials such as thin films, even small variations in film thickness can have a large impact on thermoelectric performance.[54]

While there are ways of improving thermoelectric properties, one parameter is not easily improved without affecting the rest negatively. As discussed earlier and displayed in Figure 8, the different thermoelectric properties are intertwined at different sublevels, which renders improving thermoelectric properties a real challenge.

3.2 The Cr-N Materials system

Transition metal nitrides have been thoroughly investigated over the years for hard and wear resistant coatings, contacts, diffusion barriers, and decorative coatings to name a few.[19,55–59] Among these transition metal nitrides, two have exhibited promising thermoelectric properties with their semiconductor behavior: scandium nitride (ScN) and chromium nitride (CrN).[8,13,59–66] One aspect that stands out for CrN is the relatively low thermal conductivity, with room temperature values around 2-4 $Wm^{-1}K^{-1}$, compared to 11-20 $Wm^{-1}K^{-1}$ for other transition metal nitrides.[9–12] Moreover, chromium and nitrogen are abundant and non-toxic elements – two characteristics making them attractive for future application.

CrN grows in the rock-salt cubic structure (NaCl B1-structure, Figure 9a). Fully stoichiometric, Cr:N ratio is 1:1, but thin films of cubic CrN can exist with a variation in stoichiometry, as well as with oxygen incorporation in nitrogen vacancies.[14,67] The other Cr-N phase, the hexagonal closed-packed (hcp) Cr_2N phase (Figure 9b), will be seen as a secondary phase if the nitrogen content is too low.[14,68] With increasing

temperature and at atmospheric pressure, CrN decomposes to Cr_2N (around 925 °C), which in turn decomposes to pure Cr (around 1100 °C). [69] There are indications that nitrogen is released at much lower temperatures under vacuum, something which can hinder high-temperature growth of stoichiometric CrN in vacuum chambers.[5] That CrN to Cr_2N decomposes under vacuum can be a challenge because as mentioned in previous chapter, a higher growth temperature is often a necessity for high crystal quality.

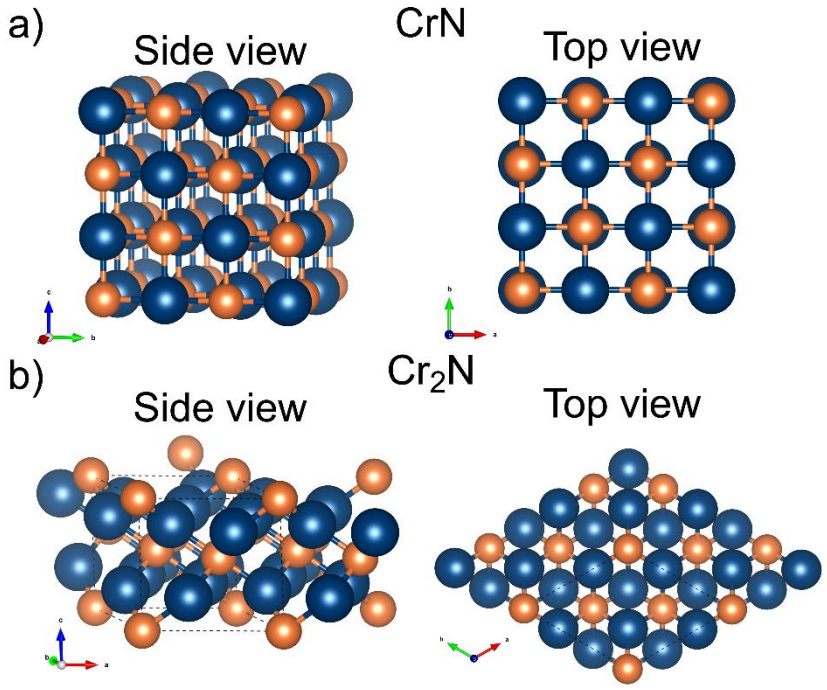

Figure 9. Crystal structure of a) CrN and b) Cr_2N. Side view and top view of both are seen. Cr atoms are colored blue and are larger than the orange N atoms (see online-version for color). The dashed lines are the unit cell (not visible for CrN due to overlap of lines and bonds). Images created in Vesta.

3.2.1 Tunability of thermoelectric properties

There are a few strategies to alter the thermoelectric properties of these Cr-N thin films. One is altering the nitrogen content. Changes in stoichiometry will have a large impact on the thermoelectric

performance of CrN. The cubic CrN materials system even changes from n- to p-type as it becomes over-stoichiometric in nitrogen.[14] This possible tuning is promising for creation of thermoelectric devices with only chromium and nitrogen (besides of course, connections in between the different legs).

Another is doping, or alloying. In principle, site substitution of Cr with isoelectronic atoms should not greatly affect the electronic properties of CrN, but the added crystal disorder should hinder phonon propagation. For instance, heavy-element doping of Mo and W have been investigated for the CrN-system, as well as Nb for the ScN-system.[61,64] Other alloying materials will influence charge carrier density, giving other means than stoichiometry for altering e.g. Seebeck coefficient and electrical conductivity.[15,44,60,63]

A third route is nanostructuring due to the two competitive phases in the Cr-N materials system. Inclusions of Cr_2N in a CrN matrix can alter its thermoelectric properties.[68,70], and a high control of secondary phase inclusion and stoichiometry of the CrN-phase could be enough for making efficient thermoelectric devices of the Cr-N materials system.

4 Characterization techniques

To characterize thin films, a range of techniques need to be employed. Structural characterization can be done by X-ray techniques, providing information on a large scale. For local structure and finer structural details, electron microscopes are applied. Compositional analysis can be done by several techniques that each have their advantages and disadvantages, including energy-dispersive X-ray spectroscopy (EDX), X-ray photoelectron spectroscopy (XPS), and ion-beam analysis. When it comes to thermoelectric measurements, there are several available techniques, but they were generally not originally designed for thin films.

4.1 Structural characterization by XRD

In 1901, Wilhelm Conrad Röntgen was awarded the first ever Nobel prize in physics for his discovery of X-rays, six years earlier. X-rays are electromagnetic waves, with a wavelength comparable to that of the interatomic distance of crystals which makes X-rays suitable for characterization of crystalline materials. X-rays interact with matter either by absorption, scattering, or refraction. The latter two are important for the techniques described in the following sections.

X-ray scattering can either be elastic (Thompson scattering) or inelastic (Compton scattering). Inelastic scattering means that energy and momentum are transferred from the incoming photon to the electron. Thus, inelastic scattering will only be a source of background noise and for diffraction techniques, it is the elastic scattering that is of interest. X-rays will strongly interact with the light electrons in atoms. As an X-ray beam reaches electrons, the electrons will start oscillating at the frequency of the incoming radiation, and itself become a source of radiation with the same frequency as the incoming beam. This radiation spreads in all directions (although, there is an angular dependency).[71] Due to the periodic nature of crystals, an interference pattern will emerge

as the incoming beam is scattered on all the atoms in the sample. There are two main aspects in achieving constructive interference. First, Bragg's law needs to be fulfilled. It states that the path-difference (2Δ) of two scattered beams must be equal to integer multiples of the wavelength. Eq. (11) and Figure 10 show the case of equal angle of the incoming and outgoing beam. Here, d is the spacing of two atomic planes, θ is the diffraction angle, n is an integer and λ is the wavelength of the beam.

$$2\Delta = 2\mathrm{d} \cdot \sin\theta = n\lambda \tag{11}$$

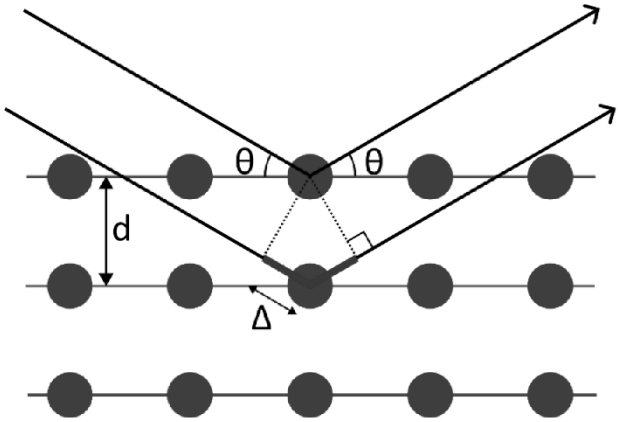

Figure 10. Illustration of Bragg's law, for constructive interference of reflections from different lattice planes. Image from Lorentzon.[28]

Second, the structure factor, *F(hkl)*, seen in eq. (12), needs to be non-zero. The structure factor determines which set of crystal planes, given by the Miller indices (h,k,l), will give rise to diffraction.

$$F(hkl) = \sum_{n=1}^{N} f_n \exp\left(i2\pi(hx_n + ky_n + lz_n)\right) \tag{12}$$

Here, f_n is the atomic form factor and x_n, y_n, z_n is the nth atom's position in the crystal cell. Stoichiometric CrN crystallizes in the cubic rock-salt structure (also known as NaCl B1). This structure can be viewed as an fcc lattice with two atoms as basis, as seen in Figure 11. For the simple case

of a monoatomic fcc crystal, there are four unique atoms in the unit cell. They are (x,y,z)=(0,0,0), (½,½,0), (½,0,½), (0,½,½). Inserting these values the structure factor for fcc crystals become as in eq. (13). Since h, k, and l are integers, it can be further simplified into eq. (14).

$$\mathrm{F}_{fcc}(hkl) = f \cdot \left(1 + \exp\left(i\pi(h+k)\right) + \exp\left(i\pi(h+l)\right) + \exp\left(i\pi(k+l)\right)\right) \tag{13}$$

$$\mathrm{F}_{\mathrm{fcc}}(hkl) = \begin{cases} 4f, & hkl\ are\ all\ even\ or\ odd \\ 0, & otherwise \end{cases} \tag{14}$$

These equations mean that for an fcc crystal, planes such as (111) and (224) can cause diffraction patterns, but not planes such as (001). For other lattices, there are different demands on *hkl*.

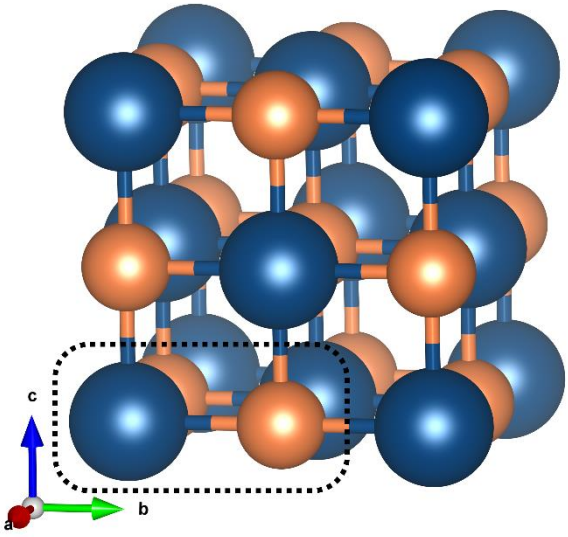

Figure 11. One unit cell of CrN. Marked is the Cr-N basis that together with the fcc-lattice creates the NaCl B1-structure.

For lab equipment, a common way to generate x-rays is by thermionic emission of electrons, which are then accelerated towards a Cu-plate over a strong electric field (typically 45 kV). Upon impact the electrons will rapidly decelerate, giving rise to Bremsstrahlung. A lot of the electrons will also remove core electrons from the copper atoms. As electrons from

higher shells fall down to the newly available lower energy state, a specific amount of energy is released. This takes the form of characteristic x-rays, with intensities much higher than that of the Bremsstrahlung. A monochromatic beam is preferred, but letting the beam pass through a monochromator greatly reduces its intensity. Instead, one often lets the beam pass through a Ni-filter. Ni, being one step to the left of Cu in the periodic table, strongly absorbs photons with slightly larger energies (shorter wavelengths) than the Cu K_α and will conveniently remove a lot of the Cu K_β-radiation while maintaining a high intensity. For materials with a high crystal quality, a diffraction doublet can be seen, due to the splitting of Cu $K_{\alpha,1}$ and $K_{\alpha,2}$. This split of K_α occurs because of spin-orbit coupling.[72]

4.1.1 Bragg-Brentano (θ-2θ)

The θ-2θ scan is the most common and basic scan. By doing a scan with both incident and reflecting angle at the same degree, one measures the crystal planes that are parallel to the surface. If the sample is polycrystalline, it is quickly shown. If there is only one peak it is likely that the sample is at least textured (and possibly epitaxial). With no reflected peaks, the sample is likely x-ray amorphous, which means that sizes of the coherent crystallographic domains in the sample are too small to yield measurable diffraction data. Although, other phenomena such as textured but tilted growth could be responsible, as well as that none of the planes parallel to the surface fulfil the requirements from the structure factor.

By comparing the diffraction data with reference powder samples (such as the vast amount of data seen in the ICDD database[73]) allows to identify the phases present in the film. A peak-shift from reference can for example be due to macroscopic stress or change in composition, and with larger grains in the film, sharper peaks in the diffractograms follows. For high quality thin films, Laue oscillations can be seen around the diffracted Bragg-Brentano peaks. Laue oscillations occur due to interference of Bragg reflections from the individual unit cells, and its

periodicity is thus a measure of the thickness of the coherently diffracting crystal.[74]

4.1.2 Pole figures

While Bragg-Brentano is useful for determining the out-of-plane orientation, it is usually also of interest to determine the in-plane orientation (texture) of the grown film, something that can be done using pole figure measurements. By keeping θ-2θ fixed and scanning along φ (rotation) and ψ (tilt), one can get *all* directions to which a certain set of planes are parallel. Pole figure measurements give no new information to randomly oriented films but are used to determine whether the film is textured or epitaxial. Recall the difference by looking at Figure 5. In fiber textured films, planes not parallel to the surface are (more or less) evenly distributed around the surface normal, and the diffraction from these planes are seen as a ring in pole figure measurements. For epitaxial films, there are a finite number of φ-values for a set of planes. For example, a cubic system with [001] growth direction will have four-fold in-plane symmetry (look at a cube from above).

Because of difference in in-/out-of-plane stresses and the fact that pole figure measurements quickly renders a lot of measurement points, the instrument needs to be set up with, in comparison to θ-2θ scans, bad optics. Otherwise, there is a chance to miss reflections even though the out-of-planes measurements have shown precisely at which angle a certain set of planes parallel to the surface is.

4.1.3 X-Ray Reflectivity

X-Ray Reflectivity (XRR) relies on refraction and reflection of x-rays in materials and is thus not a diffraction technique. It relies on destructive and constructive interference of reflections from surfaces/interlayers in the materials. The resulting plot can be used to determine the films' thickness, density, and roughness. With high crystal quality and low surface roughness, up to 200 nm thick films can be measured using this technique. In most cases, it is hard to draw conclusions on the thickness from XRR measurements if the films are thicker than around 100 nm.

The concept is similar to that of the generation of Laue oscillation, with the difference that XRR works for *any* material, and Laue oscillation relies on a thick coherently scattering domain.

4.2 Electron microscopy

Optical microscopes are useful for several applications, especially since no preparation is needed. The downside is that the wavelength of visible light (~400-750 nm) greatly limits the possible resolution. Following the findings on the duality of photons and electromagnetic radiation, de Broglie realized that the wave-particle duality must be the case for other particles as well. By accelerating electrons to 2 keV, i.e. by a voltage of 2 kV, which is a typical voltage for standard Scanning Electron Microscope (SEM), the electrons will have a wavelength of 27 pm. High-end transmission electron microscopes (TEMs) can have an acceleration voltage of 300 kV, giving the electrons a wavelength of 2.0 pm. While lenses for electrons are much worse than optical lenses, the much shorter wavelengths used in electron microscopes allow for very fine structures to be seen.

4.2.1 Scanning Electron Microscopy

SEM works by scanning a focused electron beam across the surface of the sample, while simultaneously detecting the electrons leaving every point of the surface. Different mechanisms will occur when the incoming beam strikes the surface. Most common is to detect secondary electrons (SE) emanating from the surface. These electrons give a topographic image of the surface. Often, a combination of two SE-detectors is used. A detector placed at an angle will give good depth resolution, but a detector placed directly above (as close to the electron beam as possible) will give far better spatial resolution.

SEM is easy to use and requires very little sample preparation. All that is needed is to make sure that the sample is vacuum compatible and conductive. If it is not conductive, the sample will quickly become charged and thus deflect the incoming electron beam.

Most SEMs are equipped with an Energy-Dispersive X-ray Spectroscopy (EDX or EDS) detector. The electron beam can cause electrons of the atoms in the sample to be ejected. Using a bit higher acceleration voltage compared to SEM (typically 20 kV), different types of electrons from most atoms can be ejected. In the same way as described for x-ray generation, characteristic electromagnetic radiation can be seen, yielding compositional information. EDS works best for metals and has a few percent error margin and is less suitable for light elements.

4.2.2 Transmission Electron Microscopy

While SEM allows for nm resolution, Transmission Electron Microscopy (TEM) allows for investigation down to atomic scale. As the name suggests, in TEM the electron beam is transmitted *through* the sample.[75] Since electrons react readily with atoms, the sample needs to be thin, preferably below 100 nm, which requires meticulous preparation. Normally, 1-2 samples can be prepared per day. The microscopes themselves are expensive and operating them requires a lot of practice. Despite this, TEM is routinely used in research and at universities. This is because the information given by TEM is very difficult to obtain by other methods. The downside of high resolution is that one gets very local information, and without using other, complementary techniques, it is easy to lose the meta-perspective of the samples.

Electron diffraction is often used in combination with TEM. With electron diffraction, one can get local crystallographic information, from e.g. substrate, film and interfaces.

4.3 Ion-Beam Analysis

While standard tabletop techniques such as EDS can be employed to detect and calculate metal ratios, this is not a reliable technique for light elements such as nitrogen. X-ray photoelectron spectroscopy is one method,[76] but if one also wants depth resolution, ion-beam analysis (IBA) techniques are a good choice. One large downside with IBAs is that

they require a particle accelerator. Luckily there's one at the Tandem Laboratory in Uppsala University, which is a national infrastructure allowing users from e.g. Linköping University to use these facilities.[77] The Tandem laboratory consists of, among other things, duoplasmatron and other ion sources for generating ions of virtually any element, and a Tandem accelerator, filled with SF_6 to a pressure of several bars, to allow for up to 5 MV acceleration voltage.

The following two techniques are suitable for thin films, from ~50 to a few hundred nm thick.

4.3.1 Time-of-Flight Elastic Recoil Detection Analysis

Time-of-Flight Elastic Recoil Detection Analysis (ToF-ERDA) can in principle be used to detect any element. Although, for elements heavier than $1/\sqrt{2}$ of the mass of the element of the incident beam, so-called multiple-scattering events can occur, which in turn can cause said element to be greatly overestimated. Using iodine beam, elements with atomic number of 40 (Zr) and higher are likely overestimated. The typical setup at the Tandem Laboratory for ToF-ERDA is a 36 MeV $^{127}I^{9+}$ beam, with the beam and detector set at 22.5° from the surface of the sample, for both incidence and recoil angle.

4.3.2 Rutherford Backscattering Spectroscopy

Rutherford Backscattering Spectroscopy (RBS), on the other hand, utilizes a $^{4}He^{+}$-beam. Instead of measuring recoiled species from the sample, the energy of backscattered He^{+} particles are recorded. For my measurements, the particles were accelerated to an energy of 2 MeV and were detected at an angle of 170°. RBS can accurately determine all metal ratios. The concentration of lighter elements, and especially if there are several of them, can be hard to determine by RBS alone. For thin films, a common contaminant is oxygen, even if depositions were done in a UVH system. Distinguishing oxygen from nitrogen by RBS is difficult. For transition metal nitrides, a combination of these techniques is thus preferred.

4.4 Thermoelectric measurements

Thermoelectric measurements are more niched, compared to previously described techniques which are (or should be) used in almost all research on materials science. The thermoelectric parameters are Seebeck coefficient (S), electrical conductivity or resistivity (σ, or $\rho = \sigma^{-1}$), and thermal conductivity (κ). While there are advanced industrial systems, such as ZEM3, which measures temperature-dependent Seebeck coefficient and resistivity at the same time, quick feedback is often preferred. This is where a handy homemade Seebeck bench setup is useful. Since the Seebeck coefficient is difference in voltage over difference in temperature, such a setup needs three functionalities: creating a temperature difference, measuring temperature, and measuring voltage. The schematic of the homemade setup is seen in Figure 12. By calibrating, adjusting for voltage loss/gain over the wires, and creating several measurement points over different temperature differences, this simple setup turns into a reliable technique for measuring room temperature Seebeck coefficient. The main advantages of the homemade setup are ease in handling and that it is quick. It can only measure at near room temperature and must be considered to have a bit higher inaccuracy than industrial systems. The standard deviation of measurements is usually within 10%.

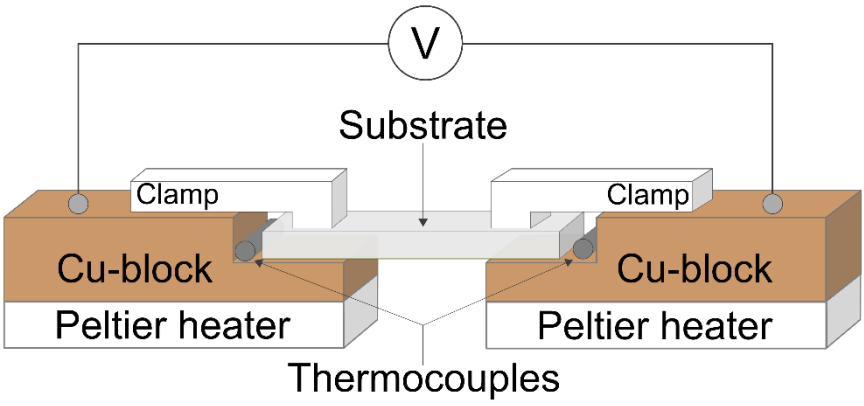

Figure 12. Simple Seebeck measurement station. Substrate is clamped in place upside down so that the film is in contact with the conductive copper blocks, which are at different temperatures thanks to the Peltier heaters.

Thermal conductivity is measured on a different setup, using methods such as 3ω-method and thermoreflectance.[78] Thermal conductivity measurement is especially tricky, and thermal conductivity is an aspect I have not yet addressed for my grown films.

4.4.1 Resistivity

From Ohm's law we get that by applying a current and measuring the voltage you can get the resistance. But, by pressing two surfaces together, a contact resistance will always arise. This contact resistance needs to be addressed if one is to measure resistivity accurately. Going from two to four probes is a way to remove the issue with contact resistance. There can be different configurations (aligning probes in a square, called van der Pauw configuration, or in a line) but the principle is the same. The four-point-probe is a technique commonly used for measuring resistivity of thin films and it works by pressing four equidistant probes against the film (Figure 13). A voltage is applied and the current is measured over the outermost probes. The center pair of probes measures the voltage. This way, no current is drawn from the probes that are measuring the voltage, and the contact resistance need not be addressed. The measured value is called sheet resistance (eq. (15)), with the somewhat unintuitive unit Ω/□ ("ohm per square").

$$R_s = \rho / d \tag{15}$$

Here, ρ is the specific resistivity and d is the film thickness. The sheet resistance is the resistance of an infinitely large and thin material. By multiplying the sheet resistance with the film thickness, which needs to be determined in other ways, and adding corrections factors for the sample size, the resistivity of the material can be found.[79] In the measurement station I have used, Jandel Model RM3000 the tips are of tungsten carbide with 100 μm radius, spaced 1 mm apart.

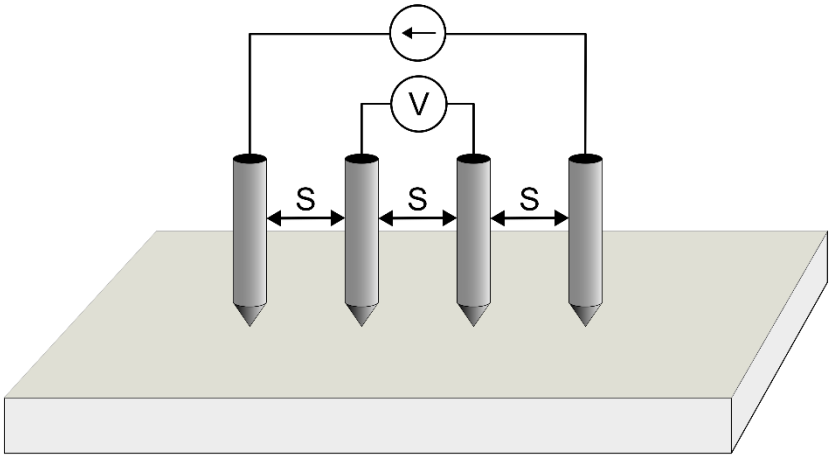

Figure 13. Four-point-probe setup for measuring resistivity.

4.4.2 ZEM3

ZEM3 is an industrial system for simultaneous measurement of Seebeck coefficient and electrical resistivity. The sample is mounted between two electrodes, one of which can be heated. Two thermocouples are placed along the sample. Both voltage and temperature difference can be measured from these. From voltage and temperature, the Seebeck coefficient can be known. Furthermore, by measuring the voltage over the thermocouples, this setup is similar to that of the four-point-probe, and electrical resistivity can be extracted. This entire setup is placed in a chamber, where the user can control both ambient gas and temperature. Keeping the measurement in an inert gas (such as He) helps avoid e.g. oxidation at elevated temperatures. Thanks to this setup, repeatable temperature-dependent measurements of both Seebeck coefficient and electrical resistivity can be performed. ZEM3 is designed for bulk materials, but with an adapter it can be used for thin films.

5 Summary and Contributions to the Field

5.1 Paper I

I investigated the effects of Mo and V addition on CrN-based thin films. I deposited the films of Cr(Mo,V)N on c-plane sapphire (Al_2O_3 (0001)) by direct current reactive magnetron sputtering. While all films grew epitaxially, Mo incorporation affected crystal structure and nitrogen content. I found that while all CrMoVN-films were under-stoichiometric in nitrogen, they largely retained the rock-salt cubic structure of stoichiometric CrN films. Addition of V assisted in stabilizing the rock-salt cubic phase, allowing for higher Mo-content than what has previously been reported. Both Seebeck coefficient and electrical resistivity decreased, in absolute values, with increasing alloying content. Although this was most likely due to the accompanying change in nitrogen content. One film, $Cr_{0.83}Mo_{0.11}V_{0.06}N_z$, showed a 70% increase in power factor ($S^2\sigma$ = 0.22 mW $m^{-1}K^{-2}$) compared to the CrN_z reference ($S^2\sigma$ = 0.13 mW $m^{-1}K^{-2}$). This work highlighted the possibility of adding additional elements for stabilizing the cubic CrN phase, but also that alloying can further hinder control of stoichiometry. Something already difficult when growing films by magnetron sputtering.

5.2 Paper II

In this paper, I investigated the thermoelectric and structural effects of high-temperature ammonia annealing on thin films of Cr-N deposited on c-plane sapphire (Al_2O_3 (0001)). Discrepancies in literature relating stoichiometry to thermoelectric properties motivated this work. Two series; single phase (cubic CrN) and mix phase (cubic CrN + hexagonal Cr_2N) were annealed. The films containing a secondary phase (Cr_2N) were converted to single phase CrN, from which an increase in thermoelectric properties followed. One of these films showed a 900% increase in power factor ($S^2\sigma$ became 0.5 mW $m^{-1}K^{-2}$) post annealing. The

single-phase films turned into ones with near insulating electrical properties, in line with theoretical work on stoichiometric CrN, straightening this question mark on previous experimental work on Cr-N. As for other material systems, ammonia annealing can be beneficial for controlling stoichiometry in lieu of meticulous deposition control. When depositing material systems such as the one in paper I, by magnetron sputtering, ammonia annealing might be the only way forward for reaching near-stoichiometry.

5.3 Outlook

There are a few aspects of **Paper I** which would be interesting to pursue. One is incorporation of lower Mo-content, to see if that would help increase nitrogen content without post-treatment. It would be interesting to repeat these series and later treat them in high-temperature ammonia annealing in an attempt to reach near-stoichiometry. If these methods would be successful in improving the power factor of said films, then thermal conductivity measurements are the next logical step. After all, reducing thermal conductivity is the main reason for introducing the heavy alloying element molybdenum.

Further alloying with cleverly chosen materials, followed not only by measurements previously mentioned, but also by measuring different transport properties such as charge carrier density and mobility[44], is one interesting way forward for CrN-alloys for thermoelectrics.

Another aspect to delve into is investigating means of controlling growth of nanoinclusions of the secondary hexagonal Cr_2N phase. Not only this, but a general control of nitrogen content while growing high quality cubic CrN films by magnetron sputtering, would be desired.

References

[1] "The Paris Agreement | UNFCCC." https://unfccc.int/process-and-meetings/the-paris-agreement (accessed Apr. 06, 2025).

[2] Forman C, Muritala IK, Pardemann R, Meyer B, "Estimating the global waste heat potential," *Renew. Sustain. Energy Rev.*, vol. 57, pp. 1568–1579, May 2016, doi: 10.1016/j.rser.2015.12.192.

[3] Maciá-Barber E, *Thermoelectric materials: advances and applications*. Singapore: Jenny Stanford Publishing, 2015. [Online]. Available: ProQuest Ebook Central, https://ebookcentral.proquest.com/lib/linkoping-ebooks/detail.action?docID=1538317.

[4] Streetman BG, Banerjee S, *Solid State Electronic Devices*, Seventh. Pearson Education Limited.

[5] Rutberg V, *Synthesis and thermoelectric properties of Cr1-xMexN (Me = Mo, V)*. 2022. Accessed: Feb. 02, 2023. [Online]. Available: http://urn.kb.se/resolve?urn=urn:nbn:se:liu:diva-188198

[6] Sootsman JR, Kong H, Uher C, D'Angelo JJ, Wu C-I, Hogan TP, Caillat T, Kanatzidis MG, "Large Enhancements in the Thermoelectric Power Factor of Bulk PbTe at High Temperature by Synergistic Nanostructuring," *Angew. Chem. Int. Ed.*, vol. 47, no. 45, pp. 8618–8622, 2008, doi: 10.1002/anie.200803934.

[7] Hu L, Zhu T, Liu X, Zhao X, "Point Defect Engineering of High-Performance Bismuth-Telluride-Based Thermoelectric Materials," *Adv. Funct. Mater.*, vol. 24, no. 33, pp. 5211–5218, 2014, doi: 10.1002/adfm.201400474.

[8] Gharavi MA, Gambino D, le Febvrier A, Eriksson F, Armiento R, Alling B, Eklund P, "High thermoelectric power factor of pure and vanadium-alloyed chromium nitride thin films," *Mater. Today Commun.*, vol. 28, p. 102493, Sep. 2021, doi: 10.1016/j.mtcomm.2021.102493.

[9] Quintela CX, Podkaminer JP, Luckyanova MN, Paudel TR, Thies EL, Hillsberry DA, Tenne DA, Tsymbal EY, Chen G, Eom C-B, Rivadulla F, "Epitaxial CrN Thin Films with High Thermoelectric Figure of Merit," *Adv. Mater.*, vol. 27, no. 19, pp. 3032–3037, 2015, doi: 10.1002/adma.201500110.

[10] Stockem I, Bergman A, Glensk A, Hickel T, Körmann F, Grabowski B, Neugebauer J, Alling B, "Anomalous Phonon Lifetime Shortening in Paramagnetic CrN Caused by Spin-Lattice Coupling: A Combined Spin and Ab Initio Molecular Dynamics Study," *Phys. Rev. Lett.*, vol. 121, no. 12, p. 125902, Sep. 2018, doi: 10.1103/PhysRevLett.121.125902.

[11] Williams WS, "The thermal conductivity of metallic ceramics," *JOM*, vol. 50, no. 6, pp. 62–66, Jun. 1998, doi: 10.1007/s11837-998-0131-y.
[12] Jankovský O, Sedmidubský D, Huber Š, Šimek P, Sofer Z, "Synthesis, magnetic and transport properties of oxygen-free CrN ceramics," *J. Eur. Ceram. Soc.*, vol. 34, no. 16, pp. 4131–4136, Dec. 2014, doi: 10.1016/j.jeurceramsoc.2014.07.030.
[13] Burmistrova PV, Maassen J, Favaloro T, Saha B, Salamat S, Rui Koh Y, Lundstrom MS, Shakouri A, Sands TD, "Thermoelectric properties of epitaxial ScN films deposited by reactive magnetron sputtering onto MgO(001) substrates," *J. Appl. Phys.*, vol. 113, no. 15, p. 153704, Apr. 2013, doi: 10.1063/1.4801886.
[14] le Febvrier A, Gambino D, Giovannelli F, Bakhit B, Hurand S, Abadias G, Alling B, Eklund P, "p-type behavior of CrN thin films via control of point defects," *Phys. Rev. B*, vol. 105, no. 10, p. 104108, Mar. 2022, doi: 10.1103/PhysRevB.105.104108.
[15] le Febvrier A, Nong NV, Abadias G, Eklund P, "P-type Al-doped Cr-deficient CrN thin films for thermoelectrics," *Appl. Phys. Express*, vol. 11, no. 5, p. 051003, Apr. 2018, doi: 10.7567/APEX.11.051003.
[16] Niklasson GA, Granqvist CG, "Electrochromics for smart windows: thin films of tungsten oxide and nickel oxide, and devices based on these," *J. Mater. Chem.*, vol. 17, no. 2, pp. 127–156, Dec. 2006, doi: 10.1039/B612174H.
[17] Mayrhofer PH, Mitterer C, Hultman L, Clemens H, "Microstructural design of hard coatings," *Prog. Mater. Sci.*, vol. 51, no. 8, pp. 1032–1114, Nov. 2006, doi: 10.1016/j.pmatsci.2006.02.002.
[18] Jehn HA, "Multicomponent and multiphase hard coatings for tribological applications," *Surf. Coat. Technol.*, vol. 131, no. 1, pp. 433–440, Sep. 2000, doi: 10.1016/S0257-8972(00)00783-0.
[19] Santecchia E, Hamouda AMS, Musharavati F, Zalnezhad E, Cabibbo M, Spigarelli S, "Wear resistance investigation of titanium nitride-based coatings," *Ceram. Int.*, vol. 41, no. 9, pp. 10349–10379, Nov. 2015, doi: 10.1016/j.ceramint.2015.04.152.
[20] Vepřek S, "The search for novel, superhard materials," *J. Vac. Sci. Technol. Vac. Surf. Films*, vol. 17, no. 5, pp. 2401–2420, 1999, doi: 10.1116/1.581977.
[21] Hübler R, Cozza A, Marcondes TL, Souza RB, Fiori FF, "Wear and corrosion protection of 316-L femoral implants by deposition of thin films," *Surf. Coat. Technol.*, vol. 142–144, pp. 1078–1083, Jul. 2001, doi: 10.1016/S0257-8972(01)01321-4.
[22] Jousten K, *Handbook of Vacuum Technology: Second, Completely Revised and Updated Edition*. John Wiley & Sons, Ltd.

[23] O'Hanlon JF, *A User's Guide to Vacuum Technology*, 1st ed. John Wiley & Sons, Ltd, 2003. doi: 10.1002/0471467162.
[24] Greczynski G, Hultman L, "A step-by-step guide to perform x-ray photoelectron spectroscopy," *J. Appl. Phys.*, vol. 132, no. 1, p. 011101, Jul. 2022, doi: 10.1063/5.0086359.
[25] Depla D, *Magnetrons, reactive gases, and sputtering*, 4th ed. 2007.
[26] Berg S, Nyberg T, "Fundamental understanding and modeling of reactive sputtering processes," *Thin Solid Films*, vol. 476, no. 2, pp. 215–230, Apr. 2005, doi: 10.1016/j.tsf.2004.10.051.
[27] Ohring M, *Materials Science of Thin Films: Depositon and Structure*. Chantilly, UNITED STATES: Elsevier Science & Technology, 2001. Accessed: Mar. 24, 2025. [Online]. Available: http://ebookcentral.proquest.com/lib/linkoping-ebooks/detail.action?docID=294629
[28] Lorentzon M, *Nanostructured TiN/ZrAlN and HfAlN Thin Films : Effect of Structure on Mechanical Properties*, vol. 1980. in Linköping Studies in Science and Technology. Licentiate Thesis, vol. 1980. Linköping: Linköping University Electronic Press, 2024. doi: 10.3384/9789180754620.
[29] Kittel, Charles, *Introduction to Solid State Physics*, 8th ed. Wiley, 2005.
[30] Stampe PA, Bullock M, Tucker WP, Kennedy RJ, "Growth of MgO thin films on M-, A-, C- and *R* -plane sapphire by laser ablation," *J. Phys. Appl. Phys.*, vol. 32, no. 15, pp. 1778–1787, Aug. 1999, doi: 10.1088/0022-3727/32/15/304.
[31] Goupil C, *Continuum Theory and Modeling of Thermoelectric Elements*. Newark, GERMANY: John Wiley & Sons, Incorporated, 2016. Accessed: Mar. 15, 2024. [Online]. Available: http://ebookcentral.proquest.com/lib/linkoping-ebooks/detail.action?docID=4205914
[32] Bell LE, "Cooling, Heating, Generating Power, and Recovering Waste Heat with Thermoelectric Systems," *Science*, vol. 321, no. 5895, pp. 1457–1461, Sep. 2008, doi: 10.1126/science.1158899.
[33] Dadhich A, Saminathan M, Kumari K, Perumal S, Ramachandra Rao MS, Sethupathi K, "Physics and technology of thermoelectric materials and devices," *J. Phys. Appl. Phys.*, vol. 56, no. 33, p. 333001, Aug. 2023, doi: 10.1088/1361-6463/acc9d0.
[34] Yadav P, Dhariwal N, Sanger A, Kang SB, Kumar V, "A review unveiling recent advances in the flexible-wearable futuristic thermoelectric device," *Nano Energy*, vol. 135, p. 110696, Mar. 2025, doi: 10.1016/j.nanoen.2025.110696.

[35] Yan Q, Kanatzidis MG, “High-performance thermoelectrics and challenges for practical devices,” *Nat. Mater.*, vol. 21, no. 5, pp. 503–513, May 2022, doi: 10.1038/s41563-021-01109-w.
[36] Snyder GJ, Toberer ES, “Complex thermoelectric materials,” *Nat. Mater.*, vol. 7, no. 2, Art. no. 2, Feb. 2008, doi: 10.1038/nmat2090.
[37] Jia N, Cao J, Tan XY, Dong J, Liu H, Tan CKI, Xu J, Yan Q, Loh XJ, Suwardi A, “Thermoelectric materials and transport physics,” *Mater. Today Phys.*, vol. 21, p. 100519, Nov. 2021, doi: 10.1016/j.mtphys.2021.100519.
[38] NASA, *Radioisotope Thermoelectric Generators (RTGs)*. [Online]. Available: https://solarsystem.nasa.gov/missions/cassini/radioisotope-thermoelectric-generator/
[39] DiSalvo FJ, “Thermoelectric Cooling and Power Generation,” *Science*, vol. 285, no. 5428, pp. 703–706, Jul. 1999, doi: 10.1126/science.285.5428.703.
[40] Goldsmid HJ, Douglas RW, “The use of semiconductors in thermoelectric refrigeration,” *Br. J. Appl. Phys.*, vol. 5, no. 11, p. 386, Nov. 1954, doi: 10.1088/0508-3443/5/11/303.
[41] Lalonde AD, Pei Y, Wang H, Jeffrey Snyder G, “Lead telluride alloy thermoelectrics,” *Mater. Today*, vol. 14, no. 11, pp. 526–532, 2011, doi: 10.1016/S1369-7021(11)70278-4.
[42] Pei Y, Lensch-Falk J, Toberer ES, Medlin DL, Snyder GJ, “High Thermoelectric Performance in PbTe Due to Large Nanoscale Ag2Te Precipitates and La Doping,” *Adv. Funct. Mater.*, vol. 21, no. 2, pp. 241–249, 2011, doi: 10.1002/adfm.201000878.
[43] Moore JP, Graves RS, “Absolute Seebeck coefficient of platinum from 80 to 340 K and the thermal and electrical conductivities of lead from 80 to 400 K,” *J. Appl. Phys.*, vol. 44, no. 3, pp. 1174–1178, Mar. 1973, doi: 10.1063/1.1662324.
[44] Zhou J, Zhu H, Song Q, Ding Z, Mao J, Ren Z, Chen G, “Mobility enhancement in heavily doped semiconductors via electron cloaking,” *Nat. Commun.*, vol. 13, no. 1, Art. no. 1, May 2022, doi: 10.1038/s41467-022-29958-2.
[45] Tian Z, Lee S, Chen G, “A Comprehensive Review of Heat Transfer in Thermoelectric Materials and Devices,” *Annu. Rev. Heat Transf.*, vol. 17, no. N/A, pp. 425–483, 2014, doi: 10.1615/AnnualRevHeatTransfer.2014006932.
[46] Joshi G, Lee H, Lan Y, Wang X, Zhu G, Wang D, Gould RW, Cuff DC, Tang MY, Dresselhaus MS, Chen G, Ren Z, “Enhanced thermoelectric figure-of-merit in nanostructured p-type silicon germanium bulk alloys,” *Nano Lett.*, vol. 8, no. 12, pp. 4670–4674, 2008, doi: 10.1021/nl8026795.

[47] Xie WJ, Yan YG, Zhu S, Zhou M, Populoh S, Gałązka K, Poon SJ, Weidenkaff A, He J, Tang XF, Tritt TM, "Significant ZT enhancement in p-type Ti(Co,Fe)Sb–InSb nanocomposites via a synergistic high-mobility electron injection, energy-filtering and boundary-scattering approach," *Acta Mater.*, vol. 61, no. 6, pp. 2087–2094, Apr. 2013, doi: 10.1016/j.actamat.2012.12.028.
[48] Minnich AJ, Dresselhaus MS, Ren ZF, Chen G, "Bulk nanostructured thermoelectric materials: current research and future prospects," *Energy Environ. Sci.*, vol. 2, no. 5, pp. 466–479, May 2009, doi: 10.1039/B822664B.
[49] Biswas K, He J, Zhang Q, Wang G, Uher C, Dravid VP, Kanatzidis MG, "Strained endotaxial nanostructures with high thermoelectric figure of merit," *Nat. Chem.*, vol. 3, no. 2, Art. no. 2, Feb. 2011, doi: 10.1038/nchem.955.
[50] Bouteiller H, Burcea R, Poterie C, Fournier D, Giovannelli F, Nyman J, Ezzahri Y, Dubois S, Eklund P, Le Febvrier A, Barbot J-F, "Improving the thermoelectric performance of scandium nitride thin films by implanting helium ions," *Commun. Mater.*, vol. 6, 2025, Accessed: Apr. 04, 2025. [Online]. Available: https://urn.kb.se/resolve?urn=urn:nbn:se:uu:diva-551514
[51] Dresselhaus MS, Chen G, Tang MY, Yang RG, Lee H, Wang DZ, Ren ZF, Fleurial J-P, Gogna P, "New Directions for Low-Dimensional Thermoelectric Materials," *Adv. Mater.*, vol. 19, no. 8, pp. 1043–1053, 2007, doi: 10.1002/adma.200600527.
[52] Sales BC, "Novel thermoelectric materials," *Curr. Opin. Solid State Mater. Sci.*, vol. 2, no. 3, pp. 284–289, Jan. 1997, doi: 10.1016/S1359-0286(97)80116-7.
[53] Hicks LD, Dresselhaus MS, "Thermoelectric figure of merit of a one-dimensional conductor," *Phys. Rev. B*, vol. 47, no. 24, pp. 16631–16634, Jun. 1993, doi: 10.1103/PhysRevB.47.16631.
[54] Jin Q, Wang Z, Zhang Q, Zhao J, Cheng H, Lin S, Chen S, Chen S, Guo H, He M, Ge C, Wang C, Wang J-O, Gu L, Wang S, Yang H, Jin K, Guo E-J, "Structural twinning-induced insulating phase in CrN (111) films," *Phys. Rev. Mater.*, vol. 5, no. 2, p. 023604, Feb. 2021, doi: 10.1103/PhysRevMaterials.5.023604.
[55] Hultman L, "Thermal stability of nitride thin films," *Vacuum*, vol. 57, no. 1, pp. 1–30, Apr. 2000, doi: 10.1016/S0042-207X(00)00143-3.
[56] Hones P, Martin N, Regula M, L vy F, "Structural and mechanical properties of chromium nitride, molybdenum nitride, and tungsten nitride thin films," *J. Phys. Appl. Phys.*, vol. 36, no. 8, pp. 1023–1029, Apr. 2003, doi: 10.1088/0022-3727/36/8/313.

[57] Abadias G, Koutsokeras LE, Dub SN, Tolmachova GN, Debelle A, Sauvage T, Villechaise P, “Reactive magnetron cosputtering of hard and conductive ternary nitride thin films: Ti–Zr–N and Ti–Ta–N,” *J. Vac. Sci. Technol. A*, vol. 28, no. 4, pp. 541–551, Jun. 2010, doi: 10.1116/1.3426296.
[58] Ushakov SV, Navrotsky A, Hong Q-J, van de Walle A, “Carbides and Nitrides of Zirconium and Hafnium,” *Materials*, vol. 12, no. 17, p. 2728, 2019, doi: 10.3390/ma12172728.
[59] Eklund P, Kerdsongpanya S, Alling B, “Transition-metal-nitride-based thin films as novel energy harvesting materials,” *J. Mater. Chem. C*, vol. 4, no. 18, pp. 3905–3914, May 2016, doi: 10.1039/C5TC03891J.
[60] Quintela CX, Rivadulla F, Rivas J, “Thermoelectric properties of stoichiometric and hole-doped CrN,” *Appl. Phys. Lett.*, vol. 94, no. 15, p. 152103, Apr. 2009, doi: 10.1063/1.3120280.
[61] Quintela CX, Rodríguez-González B, Rivadulla F, “Thermoelectric properties of heavy-element doped CrN,” *Appl. Phys. Lett.*, vol. 104, no. 2, p. 022103, Jan. 2014, doi: 10.1063/1.4861845.
[62] Biswas B, Chakraborty S, Joseph A, Acharya S, Pillai AIK, Narayana C, Bhatia V, Garbrecht M, Saha B, “Secondary phase limited metal-insulator phase transition in chromium nitride thin films,” *Acta Mater.*, vol. 227, p. 117737, Apr. 2022, doi: 10.1016/j.actamat.2022.117737.
[63] Kerdsongpanya S, Sun B, Eriksson F, Jensen J, Lu J, Koh YK, Nong NV, Balke B, Alling B, Eklund P, “Experimental and theoretical investigation of Cr1-xScxN solid solutions for thermoelectrics,” *J. Appl. Phys.*, vol. 120, no. 21, p. 215103, Dec. 2016, doi: 10.1063/1.4968570.
[64] Tureson N, Van Nong N, Fournier D, Singh N, Acharya S, Schmidt S, Belliard L, Soni A, le Febvrier A, Eklund P, “Reduction of the thermal conductivity of the thermoelectric material ScN by Nb alloying,” *J. Appl. Phys.*, vol. 122, no. 2, p. 025116, Jul. 2017, doi: 10.1063/1.4993913.
[65] le Febvrier A, Tureson N, Stilkerich N, Greczynski G, Eklund P, “Effect of impurities on morphology, growth mode, and thermoelectric properties of (1 1 1) and (0 0 1) epitaxial-like ScN films,” *J. Phys. Appl. Phys.*, vol. 52, no. 3, p. 035302, Jan. 2019, doi: 10.1088/1361-6463/aaeb1b.
[66] Kerdsongpanya S, Alling B, Eklund P, “Phase stability of ScN-based solid solutions for thermoelectric applications from first-principles calculations,” *J. Appl. Phys.*, vol. 114, no. 7, p. 073512, Aug. 2013, doi: 10.1063/1.4818415.

[67] Suzuki T, Saito H, Hirai M, Suematsu H, Jiang W, Yatsui K, "Preparation of Cr(Nx,Oy) thin films by pulsed laser deposition," *Thin Solid Films*, vol. 407, no. 1, pp. 118–121, Mar. 2002, doi: 10.1016/S0040-6090(02)00023-8.
[68] Gharavi MA, Kerdsongpanya S, Schmidt S, Eriksson F, Nong NV, Lu J, Balke B, Fournier D, Belliard L, le Febvrier A, Pallier C, Eklund P, "Microstructure and thermoelectric properties of CrN and CrN/Cr2N thin films," *J. Phys. Appl. Phys.*, vol. 51, no. 35, p. 355302, Aug. 2018, doi: 10.1088/1361-6463/aad2ef.
[69] Ernst W, Neidhardt J, Willmann H, Sartory B, Mayrhofer PH, Mitterer C, "Thermal decomposition routes of CrN hard coatings synthesized by reactive arc evaporation and magnetron sputtering," *Thin Solid Films*, vol. 517, no. 2, pp. 568–574, Nov. 2008, doi: 10.1016/j.tsf.2008.06.086.
[70] Biswas B, Chakraborty S, Chowdhury O, Rao D, Pillai AIK, Bhatia V, Garbrecht M, Feser JP, Saha B, "In-plane Cr 2 N – CrN metal-semiconductor heterostructure with improved thermoelectric properties," *Phys. Rev. Mater.*, vol. 5, no. 11, p. 114605, Nov. 2021, doi: 10.1103/PhysRevMaterials.5.114605.
[71] Cullity, B.D., *Elements of X-RAY DIFFRACTION*. Reading, Massachusetts: ADDISON-WESLEY PUBLISHING COMPANY INC., 1956.
[72] Harris R, *Modern Physics*, Second Edition. Pearson Addison-Weasley.
[73] Gates-Rector S, Blanton T, "The Powder Diffraction File: a quality materials characterization database," *Powder Diffr.*, vol. 34, no. 4, pp. 352–360, Dec. 2019, doi: 10.1017/S0885715619000812.
[74] Miller AM, Lemon M, Choffel MA, Rich SR, Harvel F, Johnson DC, "Extracting information from X-ray diffraction patterns containing Laue oscillations," *Z. Für Naturforschung B*, vol. 77, no. 4–5, pp. 313–322, May 2022, doi: 10.1515/znb-2022-0020.
[75] Williams DB, Carter CB, *Transmission Electron Microscopy*. Boston, MA: Springer US, 1996. doi: 10.1007/978-1-4757-2519-3.
[76] Bakhit B, Primetzhofer D, Pitthan E, Sortica MA, Ntemou E, Rosen J, Hultman L, Petrov I, Greczynski G, "Systematic compositional analysis of sputter-deposited boron-containing thin films," *J. Vac. Sci. Technol. A*, vol. 39, no. 6, p. 063408, Sep. 2021, doi: 10.1116/6.0001234.
[77] Mayer M, Möller S, Rubel M, Widdowson A, Charisopoulos S, Ahlgren T, Alves E, Apostolopoulos G, Barradas NP, Donnelly S, Fazinić S, Heinola K, Kakuee O, Khodja H, Kimura A, Lagoyannis A, Li M, Markelj S, Mudrinic M, Petersson P, Portnykh I, Primetzhofer D, Reichart P, Ridikas D, Silva T, Vicente SMG de, Wang YQ, "Ion

beam analysis of fusion plasma-facing materials and components: facilities and research challenges," *Nucl. Fusion*, vol. 60, no. 2, p. 025001, Dec. 2019, doi: 10.1088/1741-4326/ab5817.
[78] Zhao D, Qian X, Gu X, Jajja SA, Yang R, "Measurement Techniques for Thermal Conductivity and Interfacial Thermal Conductance of Bulk and Thin Film Materials," *J. Electron. Packag.*, vol. 138, no. 040802, Oct. 2016, doi: 10.1115/1.4034605.
[79] Miccoli I, Edler F, Pfnür H, Tegenkamp C, "The 100th anniversary of the four-point probe technique: the role of probe geometries in isotropic and anisotropic systems," *J. Phys. Condens. Matter*, vol. 27, no. 22, p. 223201, Jun. 2015, doi: 10.1088/0953-8984/27/22/223201.

Papers

The papers associated with this thesis have been removed for copyright reasons. For more details about these see:

https://doi.org/10.3384/9789181180763

FACULTY OF SCIENCE AND ENGINEERING

Linköping Studies in Science and Technology, Licentiate Thesis No. 2017, 2025
Department of Physics, Chemistry, and Biology (IFM)

Linköping University
SE-581 83 Linköping, Sweden

www.liu.se